随焊旋转挤压控制焊接热裂纹试验分析

李　军，　杨建国，　谭　星，　方洪渊
（哈尔滨工业大学 现代焊接生产技术国家重点实验室，哈尔滨　150001）

李　军

摘　要：介绍了随焊旋转挤压法的基本工作原理及其对焊接残余变形的控制效果. 以高强铝合金 2A12-T4为研究材料，对随焊旋转挤压控制焊接热裂纹进行了试验研究和机理分析. 结果表明，在合适的工艺参数下，该方法能够有效抑制铝合金焊接热裂纹的产生和扩展. 挤压头与焊枪的距离和其对工件的垂直压力是决定焊接热裂纹控制效果的两个重要参数. 随焊旋转挤压控制焊接热裂纹的机理是基于对起弧端热裂纹的压合和对焊件回转变形的拘束作用.

关键词：随焊旋转挤压；铝合金；焊接；热裂纹
中图分类号：TG407　　文献标识码：A　　文章编号：0253-360X(2010)12-0045-04

0　序　　言

由于具有低密度和优良的力学性能，铝合金材料被越来越多地应用于很多重要的制造领域，如汽车、航空和军工产品的生产[1]. 但铝合金焊接时经常出现热裂纹[2-4]，一是由于铝合金大多为共晶型合金，脆性温度区间范围较大，当易熔共晶呈薄膜状分布于晶界上时，就会破坏金属的晶间结合力，从而增加了铝合金的热裂倾向；二是加热过程中铝合金的线膨胀系数大约比铁大一倍，而其凝固时的收缩率又比铁大两倍，铝合金的这种特性会使熔池后方位于脆性温度区间金属产生较大的拉伸应变. 焊接热裂纹是焊接生产中比较常见的严重缺陷之一，它大大降低了结构的使用性能，甚至造成整个构件的报废[5]. 随焊旋转挤压（welding with trailing rotating extrusion，WTRE）是为了提高铝合金薄板焊件的焊接质量而提出的一种焊中控制新方法，试验结果表明该方法在降低铝合金焊接变形上具有显著的效果[6]，但其在焊接热裂纹控制的研究上还是空白. 因此，文中开展了随焊旋转挤压对铝合金焊接热裂倾向影响的研究，为该工艺在焊接生产中的实际应用提供借鉴.

1　随焊旋转挤压法

随焊旋转挤压是一种焊中控制方法，其工作原理如图 1所示. 工作时，固定于夹具中的薄板工件保持水平运动，工作端为圆柱状的挤压头位于电弧后方一定距离处对焊缝和近缝区金属实施旋转挤压，其所产生的纵向延展能够减小焊缝区域的纵向残余拉应力水平，从而达到降低焊接变形的目的. 图 2为 2A12-T4铝合金 WTRE焊件与常规焊件的残余变形对比，焊件尺寸为 270 mm×130 mm×2 mm.

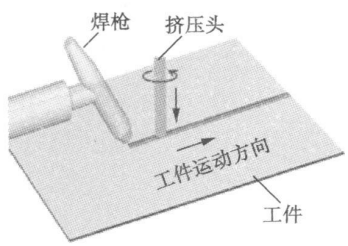

图 1　WTRE 工作原理
Fig. 1　Schematic diagram of WTRE

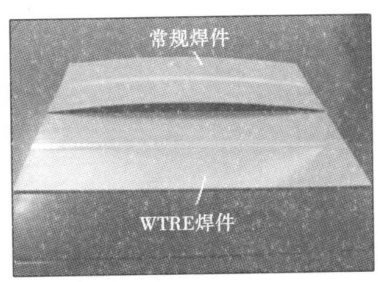

图 2　WTRE 焊件与常规焊件的残余变形对比
Fig. 2　Comparison of residual distortion between WTRE weldment and conventional weldment

收稿日期：2009-07-09
基金项目：中俄政府间科技合作资助项目（2007DFR70070）

可以看到, WTRE法控制铝合金薄板焊件残余变形的效果非常明显,经测量,常规焊件的最大纵向挠度为 6.12 mm,而 WTRE焊件为 0.24 mm,仅为常规焊件变形量的 3.92%.

2 WTRE控制焊接热裂纹试验

2.1 试验方法

试验材料选用厚度为 2 mm的 2A12T4铝合金板,试件尺寸及起弧点和收弧点位置如图 3所示. 焊接方法采用 TIG焊不填丝表面熔敷方式,焊接电流为 130 A,电弧电压为 12 V. 试验时工件置于刚性夹具的底板和压板之间 (图 4),压板对试件的拘束距离为 30 mm,夹紧螺栓扭矩为 15 N·m. 选用工作端直径为 14 mm,倒角为 R1.5 mm的挤压头 (图 5),工作时挤压头的转速为 280 r/min,工件的

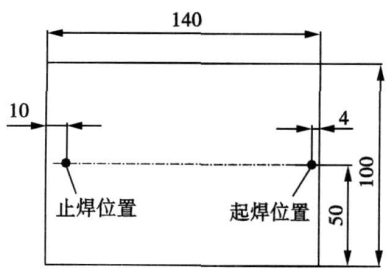

图 3 试件尺寸及起弧点和收弧点位置(mm)

Fig. 3 Dimensions of test pieces and positions of arc-starting point and arc-blowout point

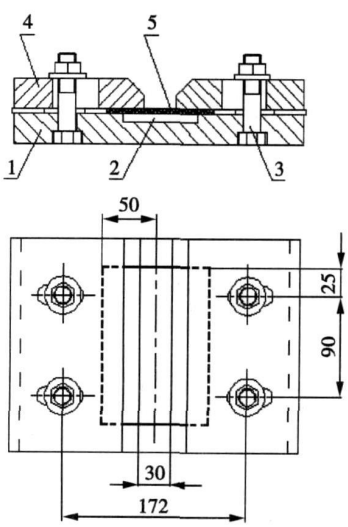

1. 底板 2. 不锈钢垫板 3. 夹紧螺栓 4. 压板 5. 工件

图 4 刚性焊接夹具及试件的夹持位置(mm)

Fig. 4 Schematic diagram of rigid welding fixture and clamping position of test piece

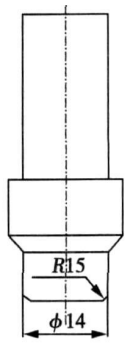

图 5 挤压头的形状和尺寸(mm)

Fig. 5 Figure and dimensions of extrusion tool

行走速度为 285 mm/min.

试验采用两种方案,一是保持挤压头对焊件的垂直压力不变,考察挤压头与焊枪的距离 (杆枪距) 对焊接热裂倾向的影响;二是保持杆枪距不变,考察挤压头对焊件的垂直压力对焊接热裂倾向的影响.

以裂纹率 H_c(%)作为热裂倾向的评定指标,表示为

$$H_c(\%) = I_{hc}/I_T$$

式中: I_{hc}为热裂纹长度; I_T为焊道长度. 为减少试验误差,对应于每组试验参数采用 3个平行试样,然后取其平均值.

2.2 试验结果

图 6为挤压头垂直压力为 1.8 kN时杆枪距对焊接热裂纹率的影响. 图 6中显示,当杆枪距为 15 mm时,焊缝起弧端无热裂纹出现;杆枪距为 18 mm时,热裂纹率小于 1%;当杆枪距增至 22 mm时,焊缝上出现明显热裂纹;随着杆枪距进一步加大,热裂纹率迅速增加,当杆枪距为 30 mm时,WTRE焊件的热裂纹率已经接近于常规焊件. 图 7为对应于不同杆枪距的 WTRE焊件与常规焊件的热裂纹长度比较.

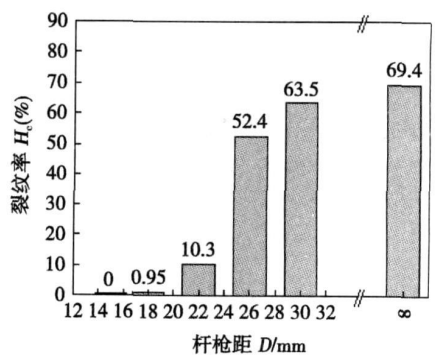

图 6 杆枪距对焊接热裂纹率的影响

Fig. 6 Influence of distance between extrusion tool and welding gun on H_c

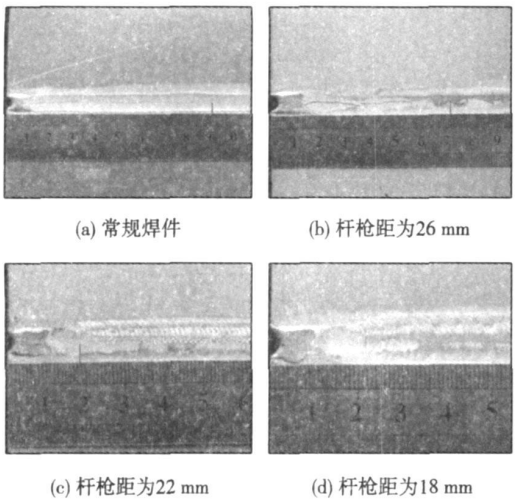

图 7　不同杆枪距下 WTRE焊件与常规焊件的热裂纹长度比较

Fig. 7　Comparison of welding hot cracks between conventional weldment and WTRE weldments treated with different distance between extrusion tool and welding gun

图 8为杆枪距为 22 mm时挤压头对焊件的垂直力对焊接热裂纹率的影响. 结果表明，挤压头对焊件的垂直力是决定焊接热裂纹控制效果的另一个重要参数. 当垂直力为 1.4 kN时，试件的热裂纹率为 24.6%，随着垂直力的增加，热裂纹率逐渐变小，当垂直力为 2.5 kN时，试件的热裂纹率只有 4.8%.

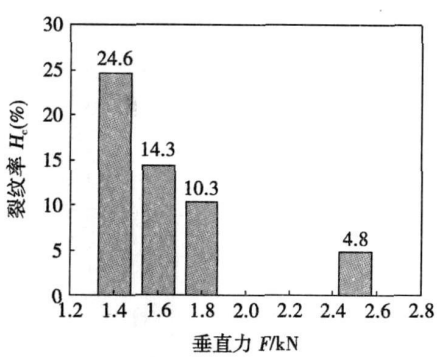

图 8　垂直压力对焊接热裂纹率的影响

Fig. 8　Influence of vertical force exerted on weldments on H_c

3　WTRE控制焊接热裂纹机理分析

热裂纹试验结果表明，当工艺参数取值适当时，WTRE法能够有效抑制焊接热裂纹的产生和扩展. 焊接开始后，熔池附近金属加热膨胀受到拘束会形成两个明显的压应力区[7]，这两个压应力区的存在会使焊接工件产生回转变形（图 9），在回转变形的带动下，位于脆性温度区间（brittle temperature range，BTR）的焊缝金属将产生拉伸应变 ε_1. 同时，由于焊缝金属在冷却过程中的凝固收缩和热收缩以及近缝区金属的热收缩，位于 BTR区间的焊缝金属还会产生拉伸应变 ε_2. ε_1 与 ε_2 之和便构成了可能导致焊缝起弧端开裂的拉伸应变 ε.

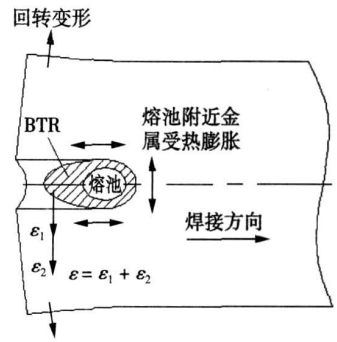

图 9　BTR区间焊缝金属拉伸应变的产生机制示意图

Fig. 9　Schematic diagram of production mechanism of tensile strain in weld metal at brittle temperature range

起弧端金属经历加热熔化并冷却到 BTR区间的下限时，焊缝中心存在低熔共晶薄膜，连接强度很低，由于受到焊件回转变形和焊缝区金属冷却收缩引起的拉伸作用而开始出现热裂纹. 但 BTR区间金属具有温度高、塑性好、粘滞性大的特点，如果受到挤压，已经出现的微裂纹很容易被压合. 当杆枪距为 15 mm时，溶池中心与挤压头工作端面边缘的最近距离只有 9～10 mm，当挤压头开始挤压时热裂纹尚未形成，高温液固共存金属在挤压头的强烈挤压下，结晶方向被打乱，因此不可能有热裂纹出现. 当杆枪距为 18 mm时，挤压头工作端面边缘恰好作用在温度靠近 BTR区间下限的焊缝金属上，已萌生的裂纹尚未扩展便被压合，因此此情况下只能在起弧端尾部观察到非常细小的微裂纹. 当杆枪距为 22 mm时，根据有限元模拟结果[7]，挤压头工作端面下的焊缝金属温度在 310～380 ℃之间，此温度下进行挤压，已经出现的热裂纹不能被压合，但由于挤压头与工件之间的摩擦系数较大，当已开裂的焊缝由于焊件回转变形而向两侧张开时，挤压头就会对这部分金属产生与其运动方向相反的摩擦力，阻碍焊件的回转变形，导致位于 BTR区间的裂纹尖端金属产生的拉伸应变 ε_1 较小，因此该参数下 WTRE焊件的热裂纹长度要明显短于常规焊件. 当杆枪距增至 26 mm以上时，挤压头下方金属的硬度已较高，挤压头与工件表面之间的摩擦力已难以拘束焊件的回转变

形,这样位于 BTR区间的焊缝中心金属就会承受较大的横向拉应力,故 WTRE工艺在杆枪距较大时控制热裂纹的效果不好.

垂直力对热裂纹控制效果的影响同样可以从拘束焊件回转变形的角度来分析. 当杆枪距为 22 mm 时,挤压头下方金属温度较高,且焊接工件与挤压头工作端面之间的摩擦系数较大,只要挤压头对焊件的垂直力足够大,且下压及时,起弧端刚萌生的热裂纹就会因为扩展驱动力不足而无法进一步扩展. 但如果垂直力不足,不能对焊件回转变形施加有效的拘束作用,则在焊件回转变形和焊缝及其邻近区域金属冷却收缩的共同作用下,热裂纹就会继续扩展,此时热裂纹的扩展程度除了受夹具拘束状态的影响,还取决于挤压头垂直力的大小,即取决于挤压头对焊件回转变形的拘束程度. 垂直力越大, BTR区间焊缝金属因焊件回转变形而产生的横向拉伸应变越小,故热裂纹的最终扩展长度就会短一些,反之,就会长一些.

4 结 论

(1)随焊旋转挤压不仅能显著降低铝合金薄板焊件的残余变形,还能起到防热裂的作用.

(2)在合适的工艺参数下,随焊旋转挤压能够有效抑制铝合金焊接热裂纹的产生和扩展,其控制焊接热裂纹的机理是基于对起弧端热裂纹的压合和对焊件回转变形的拘束作用.

(3)挤压头与焊枪的距离和其对工件的垂直力是影响焊接热裂纹控制效果的两个重要参数.

参考文献:

[1] Cicala E, Duffet G, Andrzejewski H, et al. Hot cracking in Al-Mg-Si alloy laser welding operating parameters and their effects [J]. Materials Science and Engineering A, 2005, 395(1-2): 1-9.

[2] Senkara J, Zhang H. Cracking in spot welding of aluminum alloy AA5754[J]. Welding Journal, 2000, 79(7): 194s-201s.

[3] Shimizu S, Yamanaka E, Okuda H. Study on cracking in electron beam welding of A6061[J]. Welding International, 2001, 15(10): 776-782.

[4] Gupta R K, Narayan Murty S V S. Analysis of crack in aluminium alloy AA2219 weldment[J]. Engineering Failure Analysis, 2006, 13(8): 1370-1375.

[5] 刘伟平. 反应变法防止高强铝合金 LY12CZ焊接热裂纹的研究[D]. 哈尔滨:哈尔滨工业大学, 1989.

[6] 方洪渊, 李 军, 杨建国, 等. 铝合金随焊控制焊接应力与变形的几种新方法[J]. 焊接, 2009(7): 55-60.
Fang Hong-yuan, Li Jun, Yang Jian-guo, et al. Several new in-process control methods for the welding of aluminum alloy thin-plate structures[J]. Welding & Joining, 2009(7): 55-60.

[7] 李 军. 随焊旋转挤压控制铝合金薄板焊接应力变形及防热裂研究[D]. 哈尔滨:哈尔滨工业大学, 2009.

作者简介:李 军,男,1973年出生,博士. 主要从事焊接结构可靠性与钎焊材料和工艺方面的研究工作. 发表论文 10余篇.

Email: lijun20066002@sina.com

WANG Feng, SONG Yonglun, ZHANG Jun (College of Mechanical and Electrical Engineering, Beijing University of Technology, Beijing 100124, China). p. 37—40, 44

Abstract: The influence of welding parameters (pressure and current) on the size of nugget and heat affect zone is obtained by analysing the microstructure of the nugget of the high-strength aluminum spot welding, the correlation between the parameters and the microstructure is obtained too, and the detailed influence of the little variation of the welding parameters and the less distinct change of the signals on welding nugget quality is observed, which lay a foundation for the further study of precise control of the spot welding process. The building model and the simulation of spot welding are achieved through finite element analysis software SYSWELD, and the relationship between the electrode pressure, welding current and nugget size is studied respectively.

Key words: high-strength aluminum spot welding; microstructure analyzing; finite element simulation

Testing study on SW-CCT diagram of 12Cr1MoV steel

HU Yanhua, CHEN Furong, XIE Ruijun, LI Haitao (College of Materials Science and Engineering, Inner Mongolia University of Technology, Hohhot 010051, China). p. 41—44

Abstract: Temperature was selected as variable to study phase transformation in weld metal of 12Cr1MoV steel and realized in-situ detection of temperature in weld metal. The maximum temperature and cooling rates during welding were acquired to form the simulation technology of 12Cr1MoV steel in weld metal, and the SW-CCT diagram of 12Cr1MoV steel were obtained by the thermal simulation equipment with extracted cooling rates. When the average cooling rate of $t_{8/3}$ is under 1.7 ℃/s, the microstructure in weld metal of 12Cr1MoV steel is ferrite (F) + perlite (P) + bainite (B); under 4.7 ℃/s, the microstructure is P+B; under 33 ℃/s, the microstructure is B; over 33 ℃/s, the microstructure is martensite (M). The optical microstructures of typical cooling rates are coincident with the test results of SW-CCT. The Vikers hardness increases with the increasing of cooling rates.

Key words: 12Cr1MoV steel; weld metal; SW-CCT diagram

Experimental investigation on controlling welding hot crack with welding with trailing rotating extrusion

LI Jun, YANG Jianguo, TAN Xing, FANG Hongyuan (State Key Laboratory of Advanced Welding Production Technology, Harbin Institute of Technology, Harbin 150001, China). p. 45—48

Abstract: The basic principle of welding with trailing rotating extrusion (WTRE) and its control effect in mitigating welding distortion are introduced. The impact of WTRE on welding hot crack of 2A12T4 aluminum alloy is investigated and analyzed. Experimental results show that with proper technological parameters, WTRE can inhibit the initiation and propagation of welding hot cracks effectively. The distance between extrusion tool and welding torch as well as the vertical force acting on the weldment are key technological parameters determining the control effect of welding hot cracking. WTRE method controls welding hot crack based on the binding to hot cracks at arc-starting end and the restraint action to externally expanded deformation of weldments.

Key words: welding with trailing rotating extrusion; aluminum alloy; welding; hot crack

Frictional and wear performance of WC-12Co/MoS_2 composite coatings by detonation-gun sprayed

ZHANG Song, ZHANG Kaixiang, HU Fang, ZHANG Chunhua, YAN Yongge (1. School of Materials Science and Engineering, Shenyang University of Technology, Shenyang 110870, China; 2. Baoshan Iron & Steel Co., Ltd., Shanghai 201900, China). p. 49—52

Abstract: To further improving the wear resistance of the WC-12Co coatings, different proportions of MoS_2 powders were added into the WC-12Co powders and a series of the WC-12Co/MoS_2 composite coatings were prepared on the Q235 steel by detonation-gun spraying. The morphology, microstructure, microhardness, friction and wear performance, and wear behavior of the WC-12Co/MoS_2 composite coatings were investigated by optical microscope, scanning electron microscopy, X-ray diffraction, microhardness tester and wear tester, separately. The results showed that the MoS_2 powders were evenly dispersed in the WC-12Co coatings. When the content of MoS_2 was 2% (wt%), the hardness and density of WC-12Co/MoS_2 composite coating were changed little, but the friction coefficient and wear rate were significantly decreased by 50% and 33% in contrast with those of the WC-12Co coatings, respectively. Both of the friction coefficient and wear rate of the WC-12Co/MoS_2 composite coatings were risen gradually by further increased the content of MoS_2 in the WC-12Co coating.

Key words: detonation-gun spraying; WC-12Co; MoS_2; composite coatings; wear performance

Fabrication of Fe-Ti-Mo-C composite coating by laser cladding

WANG Xinhong, ZHANG Ming, ZOU Zengda, QU Shiyao (1. Key Laboratory for Liquid-Solid Structural Evolution and Processing of Materials, Ministry of Education, Shandong University, Jinan 250061, China; 2. Institute of Thermal Science and Technology, Shandong University, Jinan 250061, China; 3. School of Mechanical Engineering, Shandong University, Jinan 250061, China). p. 53—56

Abstract: Fe-Ti-Mo-C composite coatings were deposited on the steel by laser melting mixture of Fe-Ti, Fe-Mo and graphite powders. The phase structure and microstructure of the coatings were investigated by X-ray diffraction, field emission scanning electron microscope and electron probe micro-analyzer. Meanwhile, the microhardness and wear properties of the coatings were also tested by means of micro Vickers and block-on-ring wear testing machine. The results showed that (Ti, Mo) C multiple carbides were formed during laser cladding process. (Ti, Mo) C carbide has typically faceted feature, but the lattice pattern of (Ti, Mo) C carbide is somewhat less than that of TiC. With an increasing of addition of Fe-Mo, the microhardness and wear resistance of the coatings increased, but the crack resistance of the coatings decreased.

Key words: multiple carbide; laser cladding; microstructure; wear properties